JOURNAL OF PETROLOGY | VOLUME 45 | NUMBER 2 | PAGES 405–414 | 2004 | DOI: 10.1093/petrology/egg099

The Role of Pre-existing Mechanical Anisotropy on Shear Zone Development within Oceanic Mantle Lithosphere: an Example from the Oman Ophiolite

KATSUYOSHI MICHIBAYASHI[1]* AND DAVID MAINPRICE[2]

[1]INSTITUTE OF GEOSCIENCES, SHIZUOKA UNIVERSITY, SHIZUOKA 422-8529, JAPAN

[2]LABORATOIRE DE TECTONOPHYSIQUE, CNRS UMR 5568, UNIVERSITÉ MONTPELLIER II, MONTPELLIER 34095, FRANCE

RECEIVED NOVEMBER 25, 2002; ACCEPTED AUGUST 12, 2003

Structural and fabric analysis of the well-exposed Hilti mantle section, Oman ophiolite, suggests that shear zone development, which may have resulted from oceanic plate fragmentation, was influenced by pre-existing mantle fabric present at the paleo-ridge. Detailed structural mapping in the mantle section revealed a gently undulating structure with an east–west flow direction. A NW–SE strike-slip shear zone cuts across this horizontal structure. The crystal preferred orientation (CPO) of olivine within the foliation is dominated by (010) axial patterns rather than more commonly observed (010)[100] patterns, suggesting that the horizontal flow close to the Moho involved non-coaxial flow. Olivine CPO within the shear zone formed at low temperature is characterized by (001)[100] patterns and a sinistral sense of shear. The olivine CPO becomes weaker with progressive mylonitization and accompanying grain size reduction, and ultimately develops into an ultra-mylonite with a random CPO pattern. The olivine [010]-axis is consistently sub-vertical, even where the horizontal foliation has been rotated to a sub-vertical orientation within the shear zone. These observations suggest that the primary mechanical anisotropy (mantle fabric) has been readily transformed into a secondary structure (shear zone) with minimum modification. This occurred as a result of a change of the olivine slip systems during oceanic detachment and related tectonics during cooling. We propose that primary olivine CPO fabrics may play a significant role in the subsequent structural development of the mantle. Thus, the structural behavior of oceanic mantle lithosphere during subduction and obduction may be strongly influenced by initial mechanical anisotropy developed at an oceanic spreading center.

KEY WORDS: *mantle lithosphere; anisotropy; shear zone; olivine CPO; Oman ophiolite*

INTRODUCTION

It is well known from experimental studies that the olivine slip systems have significantly different yield strengths (e.g. Durham & Goetze, 1977; Bai *et al.*, 1991). For polycrystalline natural samples, Wendt *et al.* (1998) showed clearly that the orientation of the compressive stress relative to the fabric of the rock strongly influences its strength, at least at low strains. Therefore, this suggests that the establishment of the olivine fabric could influence subsequent deformation: i.e. the effect of pre-existing mechanical anisotropy. In this study, we demonstrate that such an effect of mechanical anisotropy occurred in mantle rocks from the Oman ophiolite.

The mantle section of the Oman ophiolite is the largest section of upper oceanic lithosphere exposed at the Earth's surface. Extensive structural mapping of these rocks has been conducted throughout the Oman mountain range to unravel mantle processes associated with the generation of the oceanic lithosphere (e.g. Boudier & Nicolas, 1988; Nicolas *et al.*, 2000). It has been shown that the formation of oceanic mantle lithosphere at a fast-spreading ridge involves active mantle flow and intense olivine crystal preferred orientation

*Corresponding author. Telephone: +81-54-238-4788. Fax: +81-54-238-4788. E-mail: sekmich@ipc.shizuoka.ac.jp

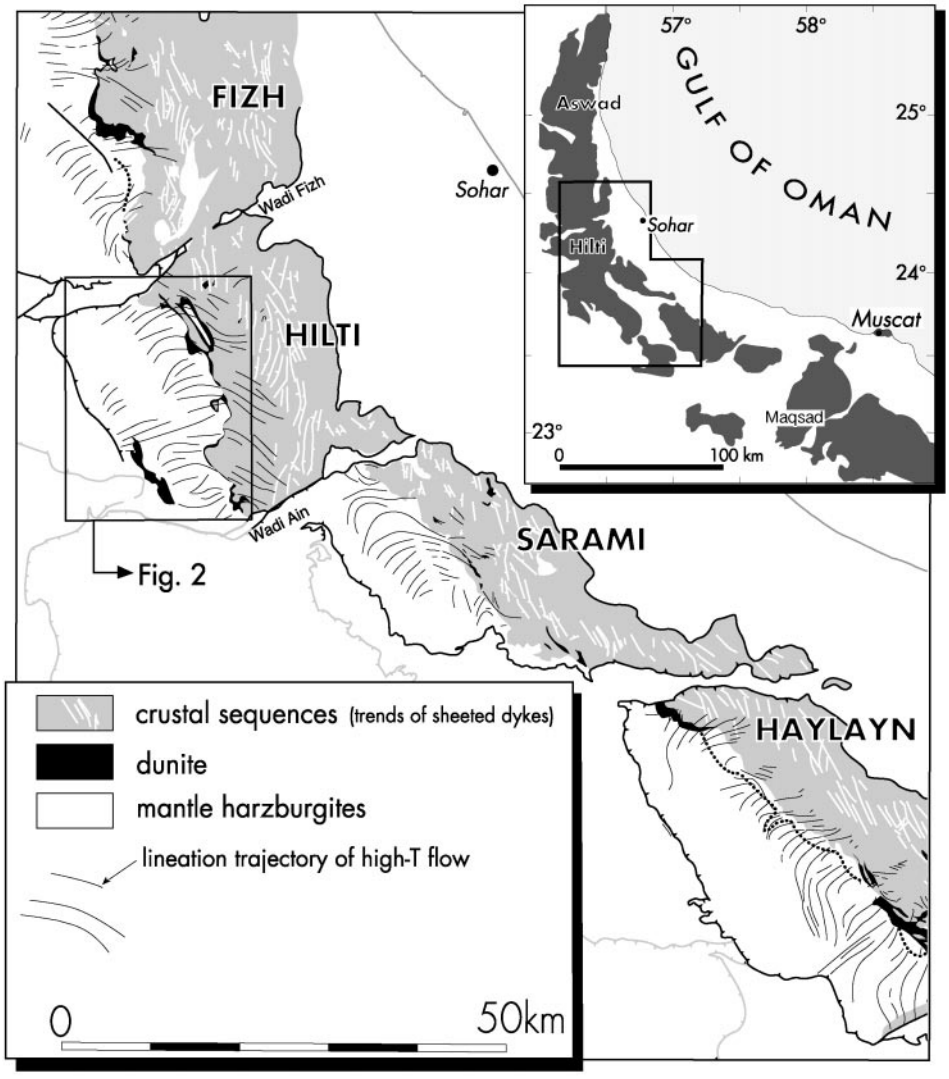

Fig. 1. Locality map and generalized geology of the northern part of the Oman ophiolite. Lineation trajectories are shown for high-temperature samples from each of the four ophiolite massifs.

(CPO) develops (e.g. Ceuleneer *et al.*, 1988; Nicolas *et al.*, 1994).

The Hilti mantle section of the northern Oman ophiolite has one of the simplest structures, where a low-temperature (low-T) sub-vertical shear zone occurs in a high-temperature (high-T) sub-horizontal mantle structure (e.g. Ildefonse *et al.*, 1995; Michibayashi *et al.*, 2000). The shear zone is thought to represent the initial stages of oceanic detachment and thrusting (Boudier *et al.*, 1988). This simple structural setting allows us to examine the role of pre-existing mechanical anisotropy on the development of a younger shear zone in the oceanic lithosphere. In this paper, we are primarily concerned with the process of strain localization as asthenosphere becomes lithosphere; thus, it is the superposition of increasing stress in the shear zone during falling temperature. As a result, olivine microstructures record a transition from coarse-grained, porphyroclastic, mylonite to ultra-mylonite textures.

GEOLOGICAL SETTINGS AND SAMPLE DESCRIPTION

The samples analyzed in this study were collected from the mantle section of the Hilti massif in the Oman ophiolite (Fig. 1). The Hilti massif records a complete ophiolite sequence consisting of (from upper to lower sections): oceanic sediments, basalt, sub-vertical sheeted dike complex, gabbro with a folded layering above a planar Moho surface, which itself overlies a thin Moho Transition Zone (MTZ) of approximately

10–100 m thickness, and finally, a vast domain of fresh peridotite (e.g. Ceuleneer *et al.*, 1988; Ildefonse *et al.*, 1995; Michibayashi *et al.*, 2000; Dijkstra *et al.*, 2002). The peridotite massif covers an area of about 25 km × 15 km between Wadi Fizh to the north and Wadi Ain to the south, whereas the western margin of the massif is cut by an east-dipping thrust.

Foliations and lineations within the peridotites are generally defined by the alignment of spinel grains. We measured these structures in the field and checked field measurements on bleached and saw-cut samples in the laboratory. We then analyzed microstructures in thin section of the *xz*-plane (i.e. perpendicular to the foliation and parallel to the lineation) of all samples to constrain the temperature of deformation. Coarse-grained (~2–4 mm) olivine with a strongly developed recovery texture is generally indicative of high-T deformation (1200–1250°C; Nicolas & Poirier, 1976) at solidus or hyper-solidus temperatures related to asthenospheric flow beneath a spreading center. Lithospheric flow at low temperature (1000–1100°C) and higher stress results in a porphyroclastic texture with varying degrees of recrystallization into fine-grained (<1 mm) neoblasts.

The orientations of lineations and foliations in the Hilti mantle section are shown in Figs 2 and 3. High-T deformation is characterized by shallow east-dipping foliation planes with an east–west flow direction (Fig. 3; Michibayashi *et al.*, 2000). However, this study has revealed that the high-T deformation structures have been overprinted by low-T deformation. In Fig. 2, the lineation trend of high-T deformation has been rotated in a sinistral sense of shear along a low-T shear zone. This rotation is strongly developed in the NE of the study area, where the high-T lineations are progressively rotated into alignment with low-T structures within the shear zone.

For the purpose of analyzing olivine fabrics, the peridotites were sampled from zones of high-T deformation near the paleo-Moho and from deeper sections of the mantle (A–L in Fig. 2). Peridotites were also sampled from areas of low-T deformation within the shear zone (a–e in Fig. 2). The high-T samples are characterized by coarse olivine grains (e.g. Fig. 4a–j), whereas the low-T samples have variable microstructures (Fig. 4a–e). Most low-T samples contain porphyroclasts, with varying degrees of recrystallization as fine-grained neoblasts (Fig. 4b–d). However, where foliations of both high-T and low-T deformation are observed at the same outcrop within the shear zone, fine-grained neoblasts are not observed. Instead, porphyroclasts are elongate sub-parallel to the low-T lineation (Fig. 4a). This sample represents the transition between the coarse, relatively equigranular texture (high-T) and the finer-grained (low-T) recrystallized microstructures. This type of microstructure has been found only in a few outcrops near the margin of the shear zone. Peridotites from the center of the shear zone have ultra-mylonitic microstructures consisting of rounded asymmetric porphyroclasts within a fine-grained olivine matrix of neoblasts (Fig. 4e).

FABRIC ANALYSIS

We collected two series of samples from the Hilti mantle section to examine CPO development within the high-T and low-T deformation series. To characterize the CPO, we determined the fabric strength and the distribution density of the principal crystallographic axes. To obtain a representative CPO of a rock, at least 100–150 grains for each phase should be measured (e.g. Ben Ismaïl & Mainprice, 1998). The rotation matrix between crystal and sample co-ordinates is used to describe the orientation $\mathbf{g}$ of a grain or crystal in sample co-ordinates. In practice, it is convenient to describe the rotation by a triplet of Euler angles, for example $\mathbf{g} = (\varphi_1, \phi, \varphi_2)$ used by Bunge (1982). The orientation distribution function (ODF), $f(\mathbf{g})$, is defined as the volume fraction of orientations with an orientation in the interval between $\mathbf{g}$ and $\mathbf{g} + d\mathbf{g}$ in a space containing all possible orientations given by

$$\Delta V/V = \int f(\mathbf{g}) d\mathbf{g}$$

where $\Delta V/V$ is the volume fraction of crystals with orientation $\mathbf{g}$, $f(\mathbf{g})$ is the texture function and $d\mathbf{g} = 1/8\pi^2 \sin\phi d\varphi_1 d\phi d\varphi_2$ is the volume of the region of integration in orientation space. Several factors will affect the degree of preferred orientation. It is well established that the strength of CPO is a function of finite plastic strain and hence the mechanical anisotropy should evolve with deformation history. To quantify the degree of CPO Mainprice & Silver (1993) used the $\mathcal{J}$ index, which is defined as

$$\mathcal{J} = \int f(\mathbf{g})^2 d\mathbf{g}.$$

The $\mathcal{J}$ index has a value of unity for a random distribution and a value of infinity for a single crystal. However, the $\mathcal{J}$ index has a maximum of about 250 for olivine in our calculations because of the truncation of the spherical harmonic series at an expansion of 22. Mainprice & Silver (1993) showed that $\mathcal{J}$ index and seismic anisotropy increase with increasing axial strain of the olivine aggregates. A more extensive study using various methods to simulate the CPO development of olivine (Tommasi *et al.*, 1999) confirms that the $\mathcal{J}$ index increases with finite plastic strain.

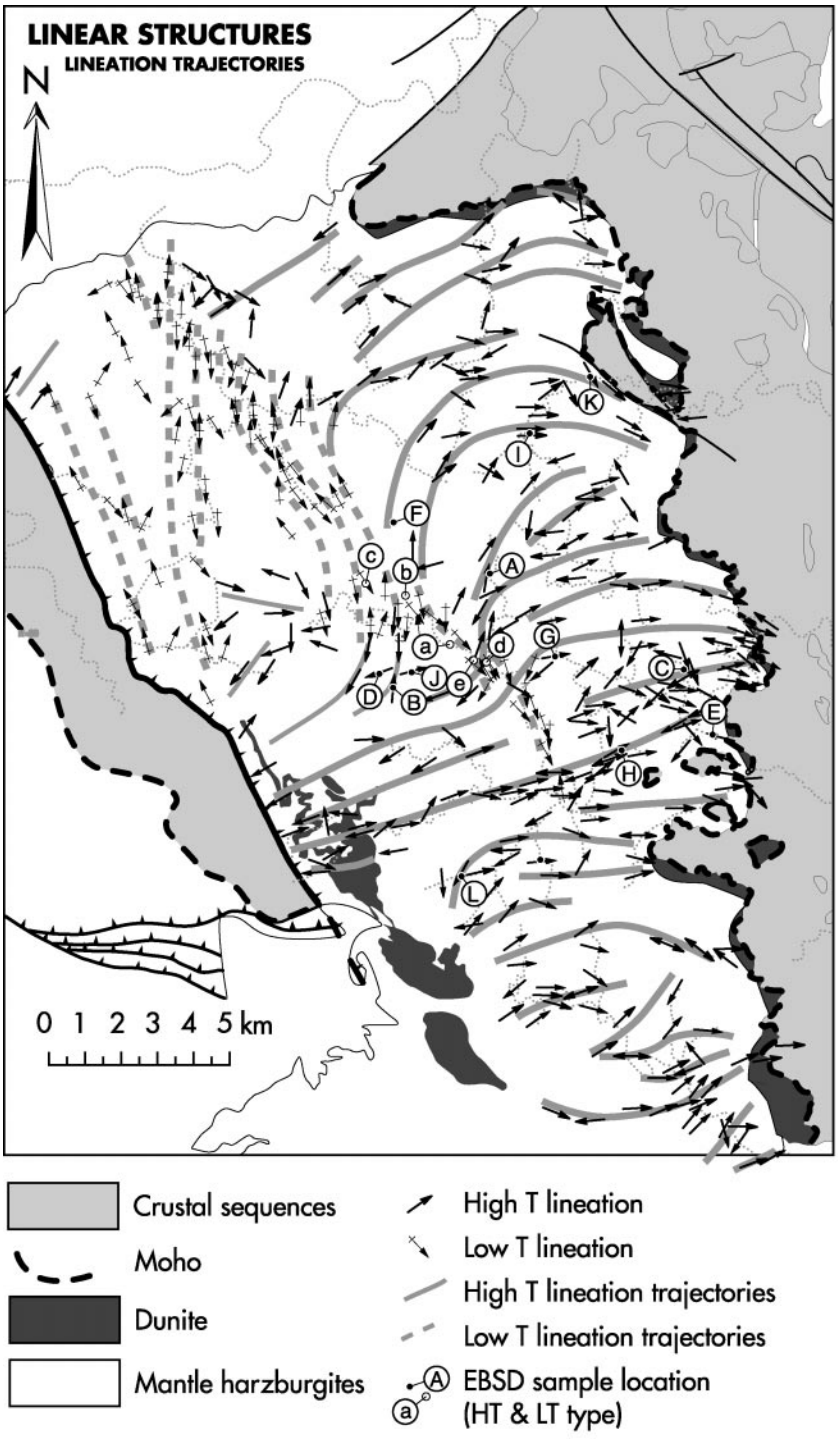

Fig. 2. Lineation trajectories within the Hilti mantle section. Although the high-T lineations are dominantly east–west, they have been progressively rotated in a sinistral sense of shear along the NW–SE-oriented low-T shear zone. Sample points for EBSD analyses are shown; high-T samples are labeled in upper case letters, and low-T samples in lower case letters. Each label is used in Figs 4–7. HT, high-T; LT, low-T.

In a similar manner the sharpness of a pole figure can be analytically defined by the $pf\mathcal{J}$ index as

$$pf\mathcal{J} = \int P_{\mathrm{hkl}}(\alpha, \beta)^2 \mathrm{d}\omega$$

where α and β are the spherical co-ordinates of the considered direction in the pole figure, $P_{\mathrm{hkl}}(\alpha, \beta)$ is the density in that direction for a given crystallographic pole defined by hkl and $\mathrm{d}\omega = 1/2\pi \sin\alpha \mathrm{d}\alpha \mathrm{d}\beta$

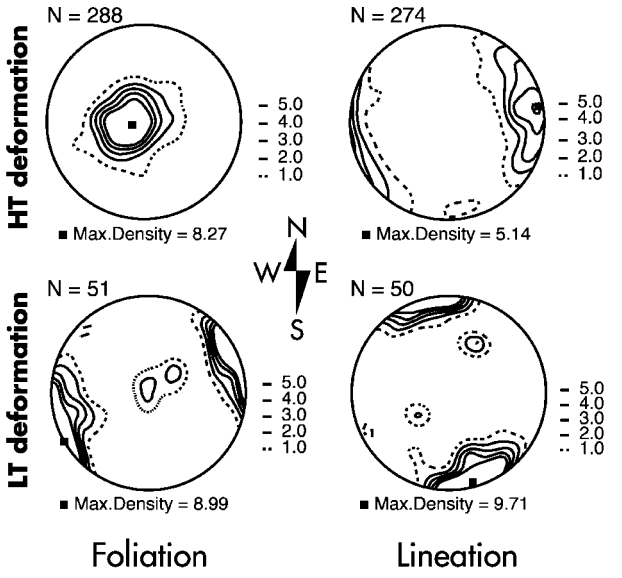

Fig. 3. Structural data from the Hilti mantle section. Shallow east-dipping foliation planes with an east–west flow direction characterize high-T deformation. Low-T deformation resulted from a sub-vertical NNW–SSE shear zone with a sub-horizontal movement.

is the volume of the region of integration. The $pf\mathcal{J}$ index has a value of unity for a random distribution and a maximum value for olivine of about 60 in the present case (which depends on the crystal symmetry and the symmetry of the crystal direction) for a single crystal of olivine. In the present case of olivine, [100]-, [010]- and [001]-axes are all two-fold rotation axes, hence the $pf\mathcal{J}$ values can be directly compared.

RESULTS

Olivine CPO patterns

Olivine CPO was measured in highly polished xz thin sections using a JEOL 5600 SEM system equipped with electron back-scattered diffraction (EBSD). Between 177 and 373 olivine crystal orientations per sample were determined and the computerized indexation of the diffraction pattern was visually checked for each orientation. The measured olivine CPO is presented on equal area, lower hemisphere projections in the structural (xz) reference frame (Figs 5 and 6). Foliation is vertical east–west and the lineation is horizontal in this plane.

Olivine CPO in high-T samples is characterized by a strong concentration of (010)-poles normal to the foliation and [100]-axes slightly oblique to the lineation (Fig. 5). The CPO occurs as one of two types: single crystal-like point maxima with [100] near the lineation and [010] near the pole to the foliation, which we will call a (010)[100] pattern (e.g. F in Fig. 5), and (010) point maxima with girdles of [100] and [001] in the foliation, which we call an axial (010) pattern (e.g. A in Fig. 5).

Olivine CPO in low-T samples is characterized by a concentration of [100]-axes parallel to the lineation, a concentration of [010]-axes sub-parallel to the y-axis, and a weak concentration of (001)-poles normal to the foliation (Fig. 6) that we will call a [100](001) pattern. The ultra-mylonite sample (e in Fig. 6) contains a random CPO of olivine grains (Fig. 6).

Intensity of olivine CPO

The degree of fabric intensity for all samples is shown in Fig. 7. For high-T samples, the $\mathcal{J}$ index ranges from 4·6 to 9·9. The spatial variation of $\mathcal{J}$ index of the ODF shows that high values ($\mathcal{J} > 7{\cdot}9$) are associated with the strong flexuring of the high-T (e.g. A, B and D in Fig. 2) and low-T (e.g. a and b in Fig. 2) lineations. The trends of the pole figure index $pf\mathcal{J}$ have more scatter, but in general follow the trends of the $\mathcal{J}$ index. However, it shows clearly that the [010]-pole figure has the highest intensity of the three axes for the high-T samples.

For low-T samples, the $\mathcal{J}$ index decreases from 10·0 to 2·6 with increasing mylonitization and accompanying grain size reduction (compare Figs 4 and 7). The $pf\mathcal{J}$ indicates that the [100]-axes become more strongly oriented than the [010]-axes.

Orientation of olivine CPO

High-T samples contain a sub-horizontal foliation. Thus, the olivine CPO in Fig. 5 indicates that both [100]- and [001]-axes lie sub-horizontally with [010]-axes vertical. For low-T samples, the foliation is sub-vertical and the lineation is sub-horizontal. Accordingly, the olivine CPO in Fig. 6 indicates that both [100]- and [001]-axes are sub-horizontal, whereas the [010]-axes are sub-vertical. This means that although the olivine CPO varies from a (010)[100] pattern in high-T samples to a (001)[100] pattern in low-T samples, the orientation has only slightly been distorted within geographic coordinates. Instead, olivine CPO has been rotated on the [010]-axis within the shear zone.

INTERPRETATION AND DISCUSSION

Olivine slip systems in high-T peridotite

The high-T olivine CPO patterns indicate slip on the (010)[100] system (Fig. 5), which is the most commonly activated slip system in naturally deformed peridotite (e.g. Nicolas & Poirier, 1976). Experimental studies have demonstrated that the (010)[100] slip

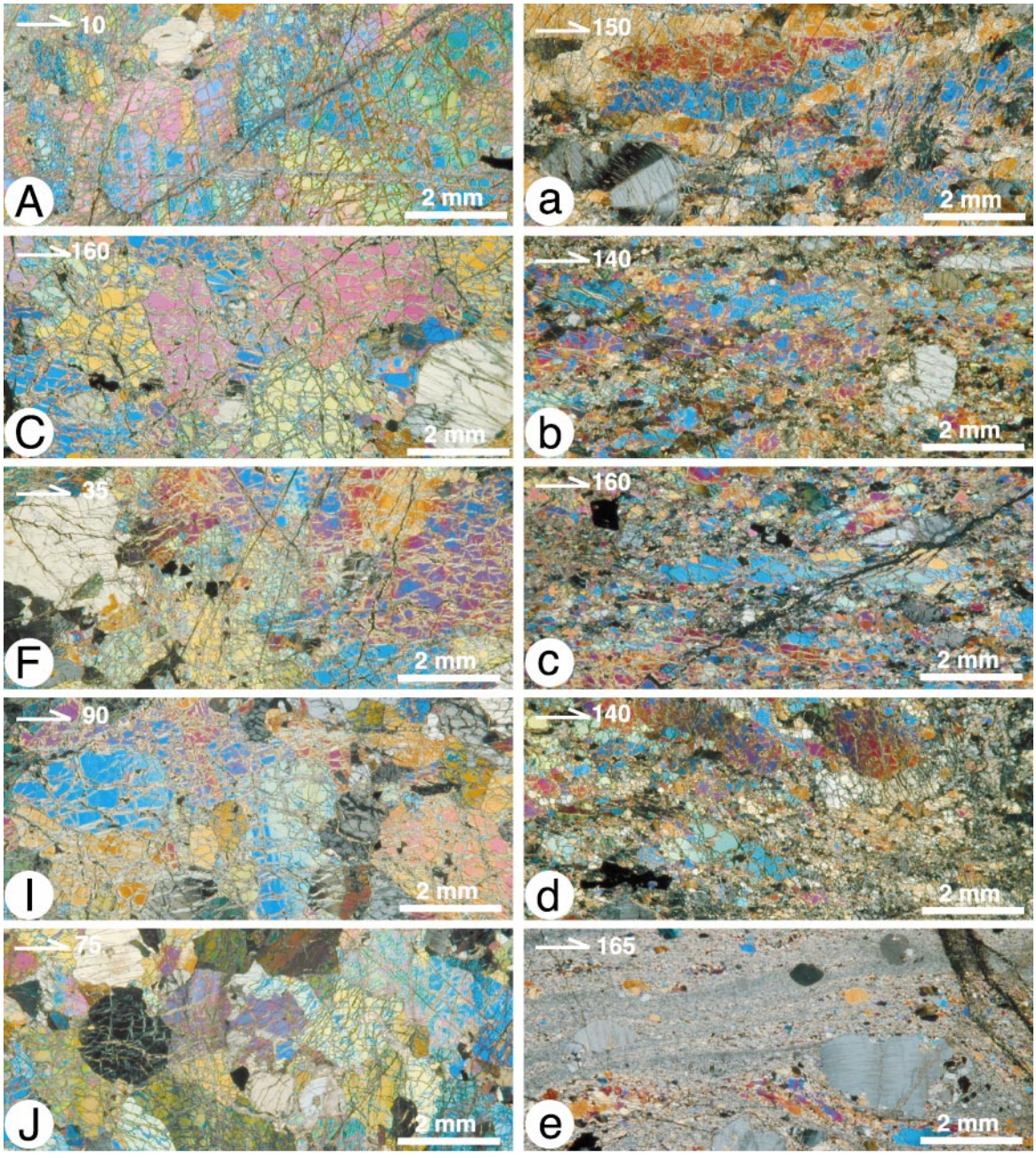

Fig. 4. Photomicrographs of peridotite samples from the Hilti mantle section. The labels are as in Fig. 2. The high-T samples are characterized by coarse olivine grains (A, C, F, I, J). The low-T samples have variable microstructures (a–e).

system is the most active at the highest temperature conditions among {0kl}[100] slip systems (e.g. Nicolas *et al*., 1973; Avé-Lallemant, 1975; Zhang & Karato, 1995; Zhang *et al*., 2000).

CPO variations were also observed from sample to sample, and some CPO patterns display axial [010] patterns. These CPO patterns can be explained in terms of the effect of finite strain in two ways. First, mantle flow may develop immediately below the Moho in response to a topographic effect in the uppermost mantle (e.g. Ildefonse *et al*., 1995). In this case, (010)[100] remains the olivine slip system, but the flow direction is not constant in orientation within the flow plane. This may be observed in the lineation data (Fig. 2), where the lineation orientation varies between samples. This could result in a diffuse concentration of [100]-axis that resembles an axial [010] pattern.

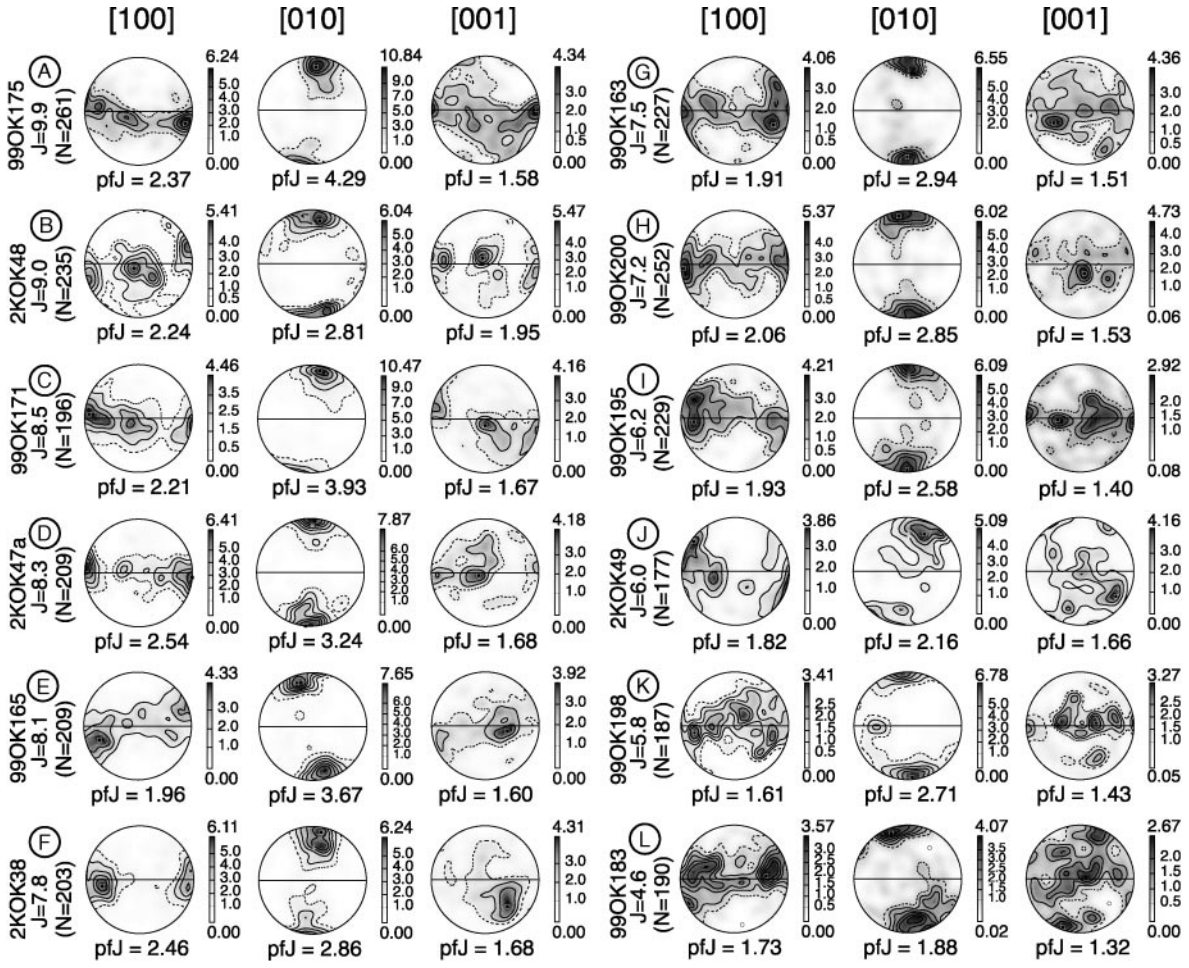

Fig. 5. Olivine CPO within high-T samples. Equal area projection, lower hemisphere. Contours in multiples of a uniform distribution (m.u.d.). Foliation is vertical (xy-plane; continuous line) and lineation (x) is horizontal within the plane of the foliation. The labels are as in Fig. 2.

The second mechanism for producing variable CPO patterns is the effect of strain path. Tommasi *et al.* (1999) showed that even though the slip system is (010)[100] active, for non-coaxial strain paths simulations produce the axial [010] pattern. The samples measured in this paper were taken from the upper oceanic mantle where sub-horizontal flow is considered to result from overturning of vertical mantle flow. In such an environment, it is possible that the subsequent horizontal flow was non-coaxial.

Alternatively, variable CPO patterns may be also influenced by variation in the amount of dynamic recrystallization. Recently, Dijkstra *et al.* (2002) showed along a section in Wadi Hilti that the recrystallized grain fraction is greatest beneath the Moho and decreases with depth into the mantle section. Dynamic recrystallization has been considered to stabilize the CPO as strain increases (e.g. Tommasi *et al.*, 2000). This may induce a progressive diffusion of CPO that will counterbalance the CPO intensification as a result of dislocation glide (Tommasi *et al.*, 2000).

Olivine slip system for low-T peridotite on pre-existing CPO pattern

The low-T olivine CPO patterns indicate (001)[100] slip in all samples except for the ultra-mylonite (Fig. 6). This CPO pattern may also result from dislocation glide on the {0kl}[100] system, although the (001)[100] system is generally regarded to be a subsidiary slip system (e.g. Tommasi *et al.*, 2000). So why did a normally subsidiary system became dominant in this shear zone?

In the shear zone described in this study, the sub-horizontal lineation, which is sub-parallel to [100]-axis concentration, strikes NW–SE (Fig. 2). It is important to note that activation of the (001)[100] slip system required only a simple rotation on the (010)-axis from

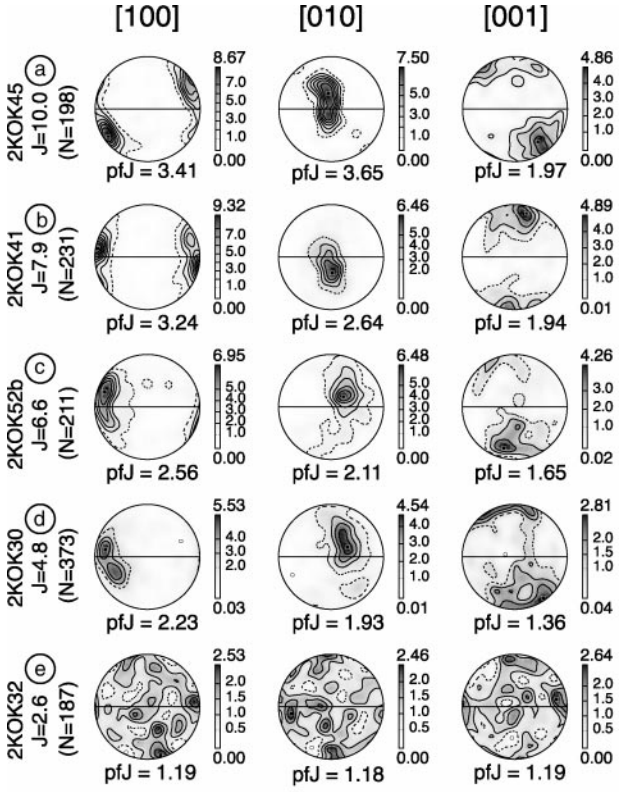

Fig. 6. Olivine CPO of low-T samples. Equal area projection, lower hemisphere. Contours in m.u.d. Foliation is vertical (xy-plane; continuous line) and lineation (x) is horizontal within the plane of the foliation. The labels are as in Fig. 2.

the pre-existing CPO patterns. Indeed, the [100]-axis would have been rotated more than 120° anticlockwise (Fig. 8). This rotation would enable the (001)[100] slip system to be dominant in olivine during deformation in the shear zone.

Experimental studies show that the (001)[100] slip system is the intermediate strength orientation at high temperature (>1150°C) and becomes active when the compression direction is parallel to [101] (e.g. Durham & Goetze, 1977; Durham *et al*., 1977; Bai *et al*., 1991; Bai & Kohlstedt, 1992). On the other hand, Phakey *et al*. (1972) showed that the compression direction parallel to [101] is weaker than that parallel to [110] or to [011] at low temperature (<1000°C).

Yanai *et al*. (1990) argued that the shear zone has been developed under east–west compression during the early stage of oceanic fragmentation. Accordingly, the direction of principal compressive stress may be statistically sub-parallel to the olivine [101]-axis during activation of the shear zone. This could activate the (001)[100] slip system in the shear zone. Even if the tectonic stress was oblique to a suitable direction for the development of this shear zone, the pre-existing anisotropy may act to modify the tectonic stress fields. However, it needs further study to better determine the direction of principal compressive stress, as this ophiolite has a complex structural history at the large scale (e.g. Nicolas *et al*., 2000).

The role of pre-existing mechanical anisotropy on shear zone development within oceanic mantle lithosphere

Although the dominant slip system active during peridotite deformation varies from (010)[100] in high-T samples to (001)[100] in low-T samples, the [010]-axis remains vertical in both cases. This occurs because subhorizontal flow in the high-T rocks was overprinted by sub-vertical flow in the low-T rocks, without disruption of the existing CPO patterns. The (010)-pole plots for low-T peridotite may record relics of high-T CPO patterns (Fig. 5). These relics suggest that the pre-existing fabric influenced development of the shear zone, and that the primary fabric was readily transformed into the secondary fabric with minimum modification following a change in the olivine slip system.

The shear zone studied in this paper is thought to represent the initial stage of oceanic detachment and thrusting (e.g. Boudier *et al*., 1988). It means that the weakest direction within the oceanic mantle lithosphere at that stage was a sub-vertical (001) plane with a horizontal [100] direction. Thus, rotation about the [010]-axis appears to lead to (001)[100] slip, and sinistral slip of the shear zone has developed sub-vertically without changing the CPO orientation (Fig. 8). In other words, it is unlikely that any other slip systems would be dominant under these conditions. It is important to note that such a weak direction may be changed if tectonic stress acts on a cooling lithospheric mantle, as the 'easy' slip system may also change depending on the lower temperature regime. We suggest that subsequent deformation could occur where pre-existing mechanical anisotropy has a suitable direction for such 'easy' slip at a lower temperature. It should be emphasized that the weakening occurs during dislocation creep deformation as a result of the anisotropy of dislocation glide, before the onset of any additional mechanical weakening caused by the onset of any significant grain boundary sliding related to the grain size reduction caused by recrystallization.

The uppermost 200 km of the mantle is thought to develop the well-defined olivine CPO through the commonly documented (010)[100] slip (e.g. Nicolas & Christensen, 1987; Mainprice *et al*., 2000). Seismic anisotropy data, such as SKS shear-wave splitting (Silver, 1996) and Pn azimuthal anisotropy (Smith & Ekström, 1999), suggest that these CPO are coherent over large distances (>100 km). Therefore,

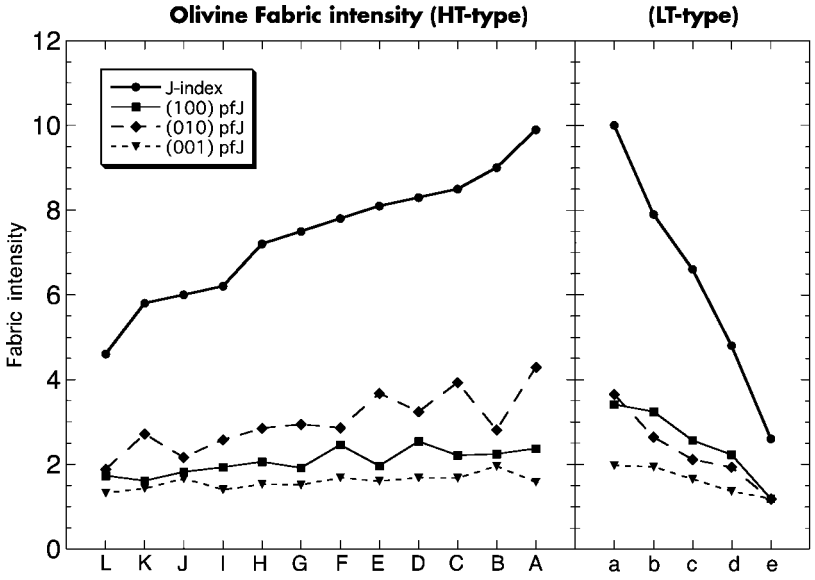

Fig. 7. Intensity of olivine CPO within high-T (HT) and low-T (LT) samples. The labels are as in Fig. 2.

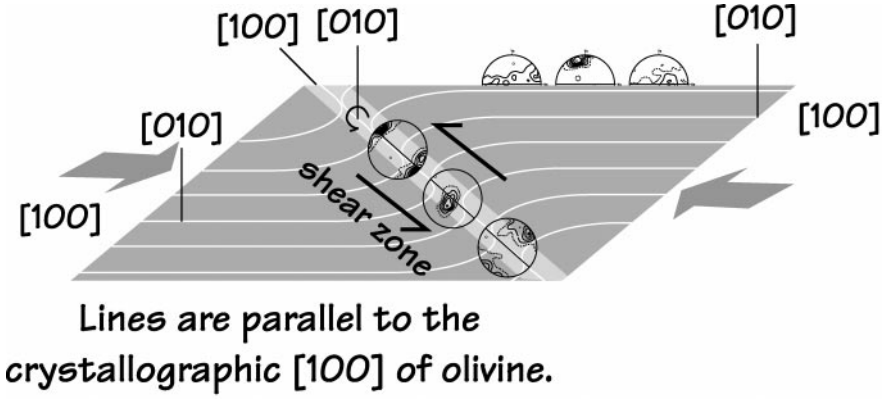

Fig. 8. Schematic diagram showing the orientation of olivine CPO between high-T and low-T deformations. Although the olivine CPO varies from a (010)[100] pattern in high-T samples to a (001)[100] pattern in low-T samples, the orientation has been only slightly distorted within geographic coordinates. Instead, the [100]-axis has been rotated more than 120° anticlockwise on the [010]-axis in a sinistral sense of shear, resulting in the activation of the (001)[100] slip system.

strain localization is likely to occur along the weakest direction within the frozen mechanical anisotropy.

For instance, the role of pre-existing mechanical anisotropy on subsequent structural development has been proposed to explain structural inheritance of continental break-up: if the preservation of well-developed olivine CPO within the lithospheric mantle generates a mechanical anisotropy at larger scales (>100 km), this may result in a directional softening that will control strain localization in the uppermost mantle (Tommasi & Vauchez, 2001). As a consequence, it suggests that the initiation of oceanic detachment as the first-step process during obduction may be dependent on the interrelations among the direction of a tectonic stress, the degree and attitude of olivine CPO, and potential 'easy' slip system as a function of temperature. The structural behavior of oceanic mantle lithosphere during subduction and obduction may be controlled by the initial mechanical anisotropy developed at an oceanic spreading center.

ACKNOWLEDGEMENTS

K. Michibayashi acknowledges F. Boudier, A. Nicolas, A. Tommasi, and other colleagues in Laboratoire de Tectonophysique for their hospitality in Montpellier, and A. Stallard of University of Canterbury, New Zealand, for improving the English of the manuscript.

The authors acknowledge Christophe Navado and Hideki Mori for their technical assistance with excellent highly polished thin sections, and M. Drury and B. Holtzman for their helpful reviews. Ministerial support given by H. Al Azri is gratefully acknowledged. This work was supported by the Centre National de la Recherche Scientifique (France) and the Japan Society of the Promotion of Science. Crystal orientation measurements were made with Laboratoire de Tectonophysique EBSD/SEM system funded by grants from CNRS/INSU, Université Montpellier II, ISTEEM and NSF #EAR-9526840 'Anatomy of an Archean craton'.

REFERENCES

Avé-Lallemant, H. G. (1975). Mechanisms of preferred orientations in olivine in tectonite peridotites. *Geology* **3**, 653–656.

Bai, Q. & Kohlstedt, D. L. (1992). High-temperature creep of olivine single crystals. 2. Dislocation structures. *Tectonophysics* **206**, 1–29.

Bai, Q., Mackwell, S. J. & Kohlstedt, D. L. (1991). High-temperature creep of olivine single crystals. 1. Mechanical results for buffered samples. *Journal of Geophysical Research* **96**, 2441–2463.

Ben Ismaïl, W. & Mainprice, D. (1998). A statistical view of the strength of seismic anisotropy in the upper mantle based on petrofabric studies of ophiolite and xenolith samples. *Tectonophysics* **296**, 145–157.

Boudier, F. & Nicolas, A. (1988). Special Issue: the ophiolite of Oman. *Tectonophysics* **151**, 1–401.

Boudier, F., Ceuleneer, G. & Nicolas, A. (1988). Shear zones, thrusts and related magmatism in the Oman ophiolite: initiation of thrusting on an oceanic ridge. *Tectonophysics* **151**, 275–296.

Bunge, H. J. (1982). *Texture Analysis in Materials Sciences*. London: Butterworths, 593 pp.

Ceuleneer, G., Nicolas, A. & Boudier, F. (1988). Mantle flow patterns at an oceanic spreading center: the Oman peridotites record. *Tectonophysics* **151**, 1–26.

Dijkstra, A. H., Drury, M. R. & Frijhoff, R. M. (2002). Microstructures and lattice fabrics in the Hilti mantle section (Oman Ophiolite): evidence for shear localization and melt weakening in the crust–mantle transition zone? *Journal of Geophysical Research* **107**, 2270–2287.

Durham, W. B. & Goetze, G. (1977). Plastic flow of oriented single crystals of olivine. 1. Mechanical data. *Journal of Geophysical Research* **82**, 5737–5753.

Durham, W. B., Goetze, G. & Blake, B. (1977). Plastic flow of oriented single crystals of olivine. 2. Observations and interpretations of the dislocation structures. *Journal of Geophysical Research* **82**, 5755–5770.

Ildefonse, B., Billau, S. & Nicolas, A. (1995). A detailed study of mantle flow away from diapirs in the Oman ophiolite. In: Vissers, R. L. M. & Nicolas, A. (eds), *Mantle and Lower Crust Exposed in Oceanic Ridges and in Ophiolites*. Dordrecht: Kluwer Academic, pp. 163–177.

Mainprice, D. & Silver, P. G. (1993). Interpretation of SKS-waves using samples from the subcontinental lithosphere. *Physics of the Earth and Planetary Interiors* **78**, 257–280.

Mainprice, D., Barruol, G. & Ben Ismaïl, W. (2000). The anisotropy of the Earth's mantle: from single crystal to polycrystal. In: Karato, S., Forte, A. M., Liebermann, R. C., Masters, G. & Stixrude, L. (eds) *Mineral Physics and Seismic Tomography: from Atomic to Global*. *Geophysical Monograph*, *American Geophysical Union* **117**, 237–264.

Michibayashi, K., Gerbert-Gaillard, L. & Nicolas, A. (2000). Shear sense inversion in the Hilti mantle section (Oman ophiolite) and active mantle uprise. *Marine Geophysical Researches* **21**, 259–268.

Nicolas, A. & Christensen, N. I. (1987). Formation of anisotropy in upper mantle peridotite: a review. In: Fuchs, K. & Froidevaux, C. (eds) *Composition Structure and Dynamics of the Lithosphere–Asthenosphere System*. *American Geophysical Union, Geodynamics Monograph Series* 111–123.

Nicolas, A. & Poirier, J. P. (1976). *Crystalline Plasticity and Solid State Flow in Metamorphic Rocks*. London: John Wiley, 444 pp.

Nicolas, A., Boudier, F. & Boullier, A. M. (1973). Mechanism of flow in naturally and experimentally deformed peridotites. *American Journal of Science* **273**, 853–876.

Nicolas, A., Boudier, F. & Ildefonse, B. (1994). Evidence from the Oman ophiolite for active mantle upwelling beneath a fast-spreading ridge. *Nature* **370**, 51–53.

Nicolas, A., Boudier, F., Ildefonse, B. & Ball, E. (2000). Accretion of Oman and United Arab Emirates ophiolite—discussion of a new structural map. *Marine Geophysical Researches* **21**, 147–179.

Phakey, P., Dollinger, G. & Christie, J. (1972). Transmission electron microscopy of experimentally deformed olivine crystals. In: Heard, H. C., Borg, I. Y., Carter, N. L. & Raleigh, C. B. (eds) *Flow and Fracture of Rocks (The Griggs Volume)*. *Geophysical Monograph*, *American Geophysical Union* **16**, 117–138.

Silver, P. G. (1996). Seismic anisotropy beneath the continents: probing the depths of geology. *Annual Review of Earth and Planetary Sciences* **24**, 385–432.

Smith, G. P. & Ekström, G. (1999). A global study of Pn anisotropy beneath continents. *Journal of Geophysical Research* **104**, 963–980.

Tommasi, A. & Vauchez, A. (2001). Continental rifting parallel to ancient collisional belts: an effect of the mechanical anisotropy of the lithospheric mantle. *Earth and Planetary Science Letters* **185**, 199–210.

Tommasi, A., Tikoff, B. & Vauchez, A. (1999). Upper mantle tectonics: three-dimensional deformation, olivine crystallographic fabrics and seismic properties. *Earth and Planetary Science Letters* **168**, 173–186.

Tommasi, A., Mainprice, D., Canova, G. & Chastel, Y. (2000). Viscoplastic self-consistent and equilibrium-based modeling of olivine lattice preferred orientations. Implications for upper mantle seismic anisotropy. *Journal of Geophysical Research* **105**, 7893–7908.

Wendt, A. S., Mainprice, D., Rutter, E. & Wirth, R. (1998). A joint study of experimental deformation and experimentally induced microstructures of pretextured peridotites. *Journal of Geophysical Research* **103**, 18205–18221.

Yanai, S., Umino, S., Ibrahim, S. O., Nakamura, Y. & Iiyama, J. T. (1990). Subduction- and collision-related emplacement of the Semail ophiolite, Northern Oman mountains. In: Malpas, J., Moores, E. M., Panayiotou, A. & Xenophontos, C. (eds) *Ophiolites: Oceanic Crustal Analogues*. *Proceedings of the Symposium 'Troodos 1987'*. Nicosia: Geological Survey Department, pp. 385–396.

Zhang, S. & Karato, S. (1995). Lattice preferred orientation of olivine aggregates in simple shear. *Nature* **375**, 774–777.

Zhang, S., Karato, S., FitzGerald, F., Faul, U. H. & Zhou, Y. (2000). Simple shear deformation of olivine aggregates. *Tectonophysics* **316**, 133–152.